Sorption and Transport in Poly(2,2-bis(trifluoromethyl)-4,5-difluoro-1,3-dioxole-*co*-tetrafluoroethylene) Containing Nanoscale Fumed Silica

Timothy C. Merkel,* Zhenjie He, and Ingo Pinnau

Membrane Technology and Research, 1360 Willow Road, Menlo Park, California 94025-1516

Benny D. Freeman

Department of Chemical Engineering, Center for Energy and Environmental Resources, University of Texas at Austin, 10100 Burnet Road, Austin, Texas 78758

Pavla Meakin and Anita J. Hill

Division of Manufacturing and Infrastructure Technology, CSIRO, Private Bag 33, Clayton, VIC 3168 Australia

Received July 10, 2003; Revised Manuscript Received August 21, 2003

ABSTRACT: The addition of nanoscale, nonporous fumed silica [FS] particles to size-selective poly(2,2-bis(trifluoromethyl)-4,5-difluoro-1,3-dioxole-*co*-tetrafluoroethylene) [AF2400] systematically increases penetrant permeability coefficients, similar to behavior previously observed in vapor-selective polyacetylenes, but contrary to results in traditional filled polymer systems. Permeability coefficients of large penetrants increase more than those of small molecules in filled AF2400, thereby decreasing the size selectivity of this polymer. AF2400 is readily plasticized by *n*-butane, whereas AF2400 containing 40 wt % FS exhibits antiplasticization behavior, suggesting that filler addition alters AF2400 to allow *n*-butane molecules to be accommodated in the polymer without significant swelling and subsequent plasticization of the matrix. Both filled and unfilled AF2400 have essentially the same gas solubility coefficients, so all of the increase in penetrant permeability in filled AF2400 is a result of increased diffusion coefficients. There is reasonable agreement between diffusion coefficients obtained from transient sorption and steady-state data, both of which increase regularly with increasing FS content. Positron annihilation lifetime spectroscopy reveals that FS addition increases the size of free volume elements in AF2400. Thermal analysis of filled AF2400 shows that FS has no detectable effect on the polymer's glass transition temperature, indicating that FS has little impact on long-range chain mobility.

Introduction

The separation of gases by selective permeation through polymer membranes has become an established unit operation that can compete successfully with traditional separation technologies.[1] To improve the competitiveness of membrane-based separations, a considerable research effort has focused on enhancing polymer selectivity and permeability. One avenue of exploration has been to add inorganic particles, such as zeolites, to polymers to combine the strong molecular sieving properties of zeolites with the desirable mechanical and processing properties of polymers.[2−4] However, efforts to reproducibly fabricate such membranes have been hampered by problems such as defects resulting from incompatibility between the polymer and the dispersed zeolite phases.[4]

Recently,[5−8] an alternate use of inorganic particles to modify transport and separation properties of polymer membranes has been identified. By adding nonporous, nanoscale fumed silica [FS] particles to certain high-free-volume, glassy polymers that are more permeable to large organic vapors than to small permanent gases, both permeability and vapor/permanent-gas selectivity increase. For example, the addition of 30 wt % FS to poly(4-methyl-2-pentyne) [PMP] simultaneously doubles mixed-gas *n*-butane/methane selectivity and increases *n*-butane permeability by a factor of 3.[5,6] The primary particle size of the FS filler used in these studies is considerably smaller than that of zeolites and molecular sieves that have previously been added to polymers to modify transport properties (10−30 nm vs ∼1 μm). The nanoscale dimensions of FS render it small enough to alter permeation and separation properties without introducing gross, selectivity-destroying defects or compromising the mechanical strength of thin polymer films at loadings of up to 50 wt %.[6,7] Because FS is nonporous, it does not permeate gas molecules as a zeolite could. Rather, it appears that for stiff-chain glasses, such as PMP, FS modifies polymer chain packing, and consequently free volume, to affect changes in polymer permeability and selectivity.[7]

In addition to PMP, we examined in detail the effect of FS addition on transport in another high-free-volume, vapor-selective polyacetylene, poly(1-trimethylsilyl-1-propyne) [PTMSP].[8] Similar to PMP, incorporation of FS into PTMSP increases penetrant permeability. However, in contrast to PMP, *n*-butane/methane selectivity decreases with increasing FS loading of PTMSP. This result is ascribed to PTMSP having larger and more interconnected free volume elements than PMP.[8] Addition of FS increases the size of these free volume elements to the point where free phase transport mechanisms that favor light gas transport, such as Knudsen diffusion, appear to become important.[8]

Here, we report permeability, solubility, and diffusion coefficients in poly(2,2-bis(trifluoromethyl)-4,5-difluoro-1,3-dioxole-*co*-tetrafluoroethylene) [AF2400] containing varying amounts of FS. AF2400, a random copolymer

10.1021/ma034975q CCC: $25.00
Published on Web 10/03/2003

containing 87 mol % of the packing-disrupting dioxole monomer, is, like PMP and PTMSP, an amorphous high-free-volume glassy material. However, unlike the polyacetylenes, it is size-selective (i.e., more permeable to light gases, such as methane, than to large vapor molecules such as *n*-butane).[9] As such, it is interesting to compare and contrast the effect of FS addition on transport in AF2400 with that in vapor-selective PMP and PTMSP. Additionally, from an applications standpoint, it is useful to determine whether nanoscale fillers can be added to a size-selective polymer to yield a mechanically robust material and whether the effect of filler on transport properties is similar to that in vapor-selective polymers. If so, filling could be a useful means of tuning transport parameters in size-selective polymers, for example, in cases where some loss in size selectivity is an acceptable tradeoff to obtain higher fluxes.

Background

Gas transport in nonporous polymer membranes proceeds by a solution-diffusion mechanism, and the permeability coefficient, P, which is the pressure and thickness normalized steady-state gas flux, is expressed as[10,11]

$$P = \left(\frac{C_2 - C_1}{p_2 - p_1}\right)\bar{D} \tag{1}$$

where $\bar{D}$ is the concentration-averaged diffusion coefficient and C_2 and C_1 are the penetrant concentrations in the polymer at the upstream (p_2) and downstream (p_1) faces of the membrane, respectively. When the downstream pressure is much less than the upstream pressure, eq 1 may be expressed in the simple form[10,11]

$$P = S\bar{D} \tag{2}$$

where S is the solubility coefficient at the upstream pressure. Permeability is frequently expressed in barrers, where 1 barrer $= 10^{-10}$ cm^3 (STP) cm/(cm^2 s cmHg).

The ideal permselectivity of a polymer film for component A relative to component B, $\alpha_{A/B}$, is defined as the ratio of their permeabilities, which in light of eq 2 may be rewritten as the product of two ratios:[10,11]

$$\alpha_{A/B} = \frac{P_A}{P_B} = \left(\frac{S_A}{S_B}\right)\left(\frac{\bar{D}_A}{\bar{D}_B}\right) \tag{3}$$

where the first term on the right-hand side is the solubility selectivity and the second is the mobility or diffusivity selectivity.

Classically, a number of theoretical expressions have been advanced to describe transport behavior in heterogeneous polymer systems.[12] Such models attempt to account for volume filling and increased diffusive tortuosity caused by the presence of filler particles. As might be anticipated, these models predict a reduction in polymer permeability with increasing nonporous filler content. Despite their simplicity, they have been found, at least qualitatively, to describe gas transport in many filled polymers.[12,13] However, models of this type are unable to predict the increased permeability observed in FS-filled PMP and PTMSP and the dependence of these properties on the primary particle size of the filler particles,[7,8] presumably because the models offer no means of accounting for changes in polymer phase permeability in the filled materials nor the possibility of an interfacial phase with transport properties different from those of the polymer and the filler.

Gas solubility in a binary system consisting of filler particles and polymer may depend on the filler concentration as well as possible particle interactions with the polymer matrix. The following additive model has previously proved useful for describing sorption in FS-filled polymers:[14]

$$S = \varphi_p S_p + (1 - \varphi_p)S_f \tag{4}$$

where S_p is solubility in the polymer matrix, S_f refers to solubility in porous fillers or on nonporous filler particles, and φ_p is the volume fraction of polymer.

Experimental Section

Film Preparation. Dense films of AF2400 and AF2400/FS nanocomposites were prepared by solution casting. AF2400 (DuPont, Wilmington, DE) was dissolved in PF5060, a perfluorinated solvent supplied by 3M (Minneapolis, MN), to prepare a 1 wt % polymer solution. A nonporous, hydrophobic grade of FS available from Cabot Corp. (Tuscola, IL), Cab-O-Sil TS-530, was added to the polymer solution. TS-530 FS has been chemically treated with hexamethyldisilazane to replace hydroxyl surface groups with hydrophobic trimethylsilyl surface groups.[15] The desired amount of FS was added to the polymer−solvent solution and physically mixed at 18 000 rpm for 10 min in a Waring two-speed commercial blender. The blended mixture was filtered, poured into a casting ring, and dried at ambient conditions until all solvent had evaporated. AF2400 and AF2400/FS nanocomposite films were solvent-free after drying for about 24 h. The films used in this study were approximately 50 μm thick as determined by a precision micrometer. Further details of the nanocomposite film preparation protocol are described elsewhere.[7]

Thermal Characterization. Thermal analysis of AF2400 and FS-filled AF2400 films was conducted with a TA Instruments (New Castle, DE) 2010 differential scanning calorimeter (DSC) connected to a computer running TA's Thermal Solutions software. DSC scans were performed in a nitrogen atmosphere at a heating rate of 20 °C/min from room temperature up to 300 °C. Film samples ranging from 10 to 12 mg were sealed in aluminum sample pans. Second scan thermograms were used to determine glass transition temperatures.

Positron Annihilation Lifetime Spectroscopy. The PALS measurements were performed in N_2 at ambient temperature using an automated EG&G Ortec fast−fast coincidence system. The timing resolution of the system was 240 ps determined using the prompt curve from a ^{60}CO source with the energy windows set to ^{22}Na events. Polymer films approximately 50 μm thick were stacked to a total thickness of 1 mm on either side of the 30 μCi ^{22}Na−Ti foil source. From 5 to 15 spectra were collected for each sample with a 1 h acquisition time required per spectrum. These results were averaged to yield mean values. The standard deviations were the population standard deviations for nine spectra, and each spectrum consisted of approximately 1 million integrated counts. The PALS parameters for the spectra did not vary as a function of contact with the radioactive source. The spectra were modeled as the sum of four decaying exponential terms using the computer program PFPOSFIT. While the PALS signatures of most polymers can be modeled using three decaying exponential terms, a four-parameter fit gave better statistical results for the materials discussed in this work. The shortest lifetime was fixed at 125 ps, which is characteristic of parapositronium self-annihilation. No source correction was used in the analysis based on a fit for pure Al standards of 169 ± 2 ps, 99.3 ± 0.3%; 820 ps, 0.7%. Only the orthopositronium (oPs) components with the longest measured lifetimes—the third (τ_3) and fourth (τ_4)—were considered further since they are ascribed to annihilations in free volume cavities of the polymer matrix.

Permeation Measurements. Pure-gas permeation properties of AF2400 and FS-filled nanocomposites were determined with a constant-pressure/variable-volume apparatus.[16] The surface area of the film was 13.8 cm^2, and gas flow rates were measured with a soap-film bubble flowmeter. Prior to each experiment, both the upstream and downstream sides of the permeation cell were purged with penetrant gas. Permeability coefficients of gases and vapors were determined in the order of increasing penetrant condensability, i.e., H_2, N_2, O_2, CH_4, n-C_4H_{10}. When steady-state conditions were achieved, the following expression was used to evaluate permeability[16]

$$P = \frac{l}{p_2 - p_1}\frac{273}{\mathrm{TA}}\frac{p_{\mathrm{atm}}}{76}\left(\frac{\mathrm{d}V}{\mathrm{d}t}\right) \quad (5)$$

where l is the film thickness, p_2 is the upstream pressure, p_1 is the downstream pressure (atmospheric pressure in this case), p_{atm} is atmospheric pressure (cmHg), A is the membrane area, T is the absolute temperature, and dV/dt is the volumetric displacement rate of the soap-film in the bubble flowmeter.

Mixed-gas permeation properties of films were determined with a feed containing 2 vol % n-butane in methane. The feed pressure in these experiments was 11.2 atm, and the permeate pressure was atmospheric. The ratio of permeate to feed flow rate, or stage cut, was always less than 1%. Under these conditions the residue and feed compositions are essentially equal. The permeate composition was determined with a gas chromatograph equipped with a thermal conductivity detector. Mixed-gas permeability coefficients for n-butane and methane were determined from the following relationship:

$$P = \frac{x_{\mathrm{perm}}l}{x_{\mathrm{feed}}p_2 - x_{\mathrm{perm}}p_1}\frac{273}{\mathrm{TA}}\frac{p_{\mathrm{atm}}}{76}\left(\frac{\mathrm{d}V}{\mathrm{d}t}\right) \quad (6)$$

where x_{feed} and x_{perm} refer to the mole fractions of components in the feed and permeate streams, respectively.

Sorption Measurements. Uptake of n-butane in AF2400, in AF2400/FS nanocomposites, and on TS-530 FS powder was measured with a Cahn RG Electrobalance (Bellflower, CA). The balance is serviced by a vacuum system and housed in an insulated box equipped with an air bath temperature regulation system. Approximately 40 mg of sample was placed on the balance and degassed under vacuum. The sample was then exposed to a fixed n-butane pressure, and mass uptake was monitored as a function of time using a computer equipped with Labtech (Andover, MA) data acquisition software. This procedure was repeated for incrementally higher n-butane pressures to obtain a sorption isotherm.

Results and Discussion

Thermal Characterization. For the filled polymers previously examined, PMP and PTMSP, it is difficult to examine the impact of FS addition on the glass transition temperature, T_g, because these polyacetylenes thermally decompose before exhibiting a glass transition. This is not the case for AF2400, which has a well-established T_g around 240 °C.[17] This fact allows us to probe the effect of FS content on long-range chain mobility in AF2400. From DSC scans, the glass transition temperature of AF2400 was 244 °C, which is within the typical range for this polymer. Subsequent scans of AF2400 films containing different loadings of FS (10, 25, and 40 wt %) showed no significant change in glass transition temperature (T_g ranged between 242 and 246 °C). This result indicates that the presence of FS particles does not measurably alter the long-range segmental dynamics important to the glass transition in AF2400. Given the nonpolar, hydrophobic nature of AF2400 and TS-530 FS, it is reasonable that interactions between the two, which might affect T_g, are very weak and that the primary impact of FS addition is on chain packing and not on chain stiffness or mobility.

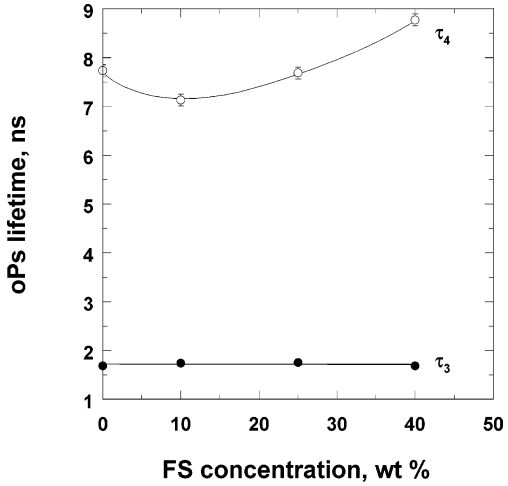

Figure 1. Effect of FS content on oPs lifetimes in AF2400. PALS spectra were collected at ambient temperature in a nitrogen environment and modeled as the sum of four decaying exponential terms using the computer program PFPOSFIT.

Previous studies on the effect of filler addition on polymer glass transition temperature show a wide variety of behavior. Most often fillers increase T_g, presumably due to interactions between the filler surface and polymer chains that restrict chain mobility.[18] For example, Iisaka and Shibayama[19] demonstrate a correlation between the heat of absorption of polymer chains on a filler surface and the associated increase in polymer glass transition temperature. Similarly, Yim et al.[20] report a direct relation between polymer−filler interaction energy and the increase in T_g for several different polymer−silica composites. However, filler addition may also decrease or have no effect on T_g. For instance, Hergeth et al.[21] report that the addition of up to 50 wt % silica to poly(vinyl acetate) and polystyrene does not change the glass transition temperature of these polymers. In addition to the strength of polymer−filler interactions, Lipatov and Fabulyak[22] suggest that polymer chain stiffness is an important factor in considering a filler's impact on T_g. In the case of rigid polymer chains, the effects of filler surface interaction on chain mobility may not be detectable. Such findings are generally consistent with our observation that the addition of nonpolar FS to nonpolar, stiff-chain AF2400 produces no measurable change in T_g.

Positron Annihilation Lifetime Spectroscopy. Figure 1 illustrates the effect of FS content on oPs lifetimes in AF2400. As mentioned previously, the longer the average lifetime of oPs probe particles in a sample, the larger the average size of free volume elements in the polymer. For most polymers, PALS spectra are described by a single oPs lifetime, τ_3. However, in high-free-volume polymers, such as AF2400, a second, longer oPs lifetime, τ_4, is often observed.[23] It has been suggested that τ_4 corresponds to large, long-lived free volume elements in such polymers.[24] The current PALS analysis of AF2400 and FS-filled AF2400 indicates that these materials possess a bimodal distribution of oPs lifetimes. On the basis of the data in Figure 1, the shorter oPs lifetimes (τ_3) appear to be nearly independent of FS concentration, whereas the longer lifetimes (τ_4) generally increase with increasing FS content. This result indicates that the addition of FS increases the size of large free volume elements in

Table 1. Permeability of Aged AF2400 Films Containing Fumed Silica[a]

	as-cast sample permeability (barrers)		aged sample permeability (barrers)	
sample	N_2	CH_4	N_2	CH_4
AF2400	340	250		
AF2400 + 10 wt % TS530	480	380	550	420
AF2400 + 40 wt % TS530	1060	1090	990	940

[a] All data are for pure gases taken at 25 °C and $\Delta p = 3.4$ atm. After the as-cast measurements for N_2 and CH_4 were conducted, the film samples were tested with *n*-butane at pressures up to the vapor pressure of this compound at room temperature. Subsequently, the films were stored in ambient atmosphere for 2.2 years prior to the second set of measurements.

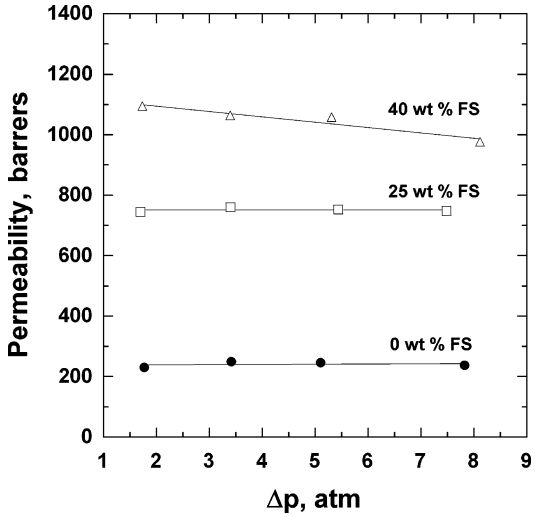

Figure 2. Methane permeability coefficients at 25 °C in AF2400 containing 0, 25, and 40 wt % FS as a function of the transmembrane pressure difference, Δp.

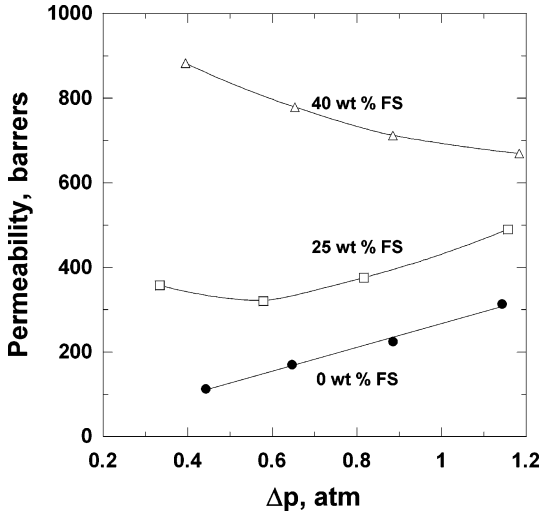

Figure 3. *n*-Butane permeability coefficients at 25 °C in AF2400 containing 0, 25, and 40 wt % FS as a function of the transmembrane pressure difference, Δp.

AF2400. A similar effect was observed when FS was added to PMP[7] and PTMSP,[8] where it was shown that the subtle increase in free volume detected by PALS resulted in significant increases in penetrant permeability and diffusion coefficients.

Permeability. Figure 2 presents methane permeability coefficients in AF2400 containing 0, 25, and 40 wt % FS at 25 °C as a function of the transmembrane pressure difference, Δp. Consistent with previous studies of AF2400,[9,25,26] the permeability of this polymer is very high relative to that of conventional glassy polymers. For example, the methane permeability coefficient in AF2400 (250 barrers at 25 °C) is orders of magnitude higher than in low-free-volume polymers, such as poly(tetrafluoroethylene) (0.74 barrer at 25 °C)[27] or polycarbonate (0.26 barrer at 35 °C).[27] Previous studies of AF2400 have reported that the methane permeability coefficient for this polymer in the vicinity of room temperature may vary from 340 to 600 barrers.[9,25,26,28] The permeability of AF2400 to methane in the present work is slightly below this range; however, given the scatter in reported permeabilities for AF2400, our result is reasonable. The exact cause of the variation in reported AF2400 permeabilities is unknown, although it has been suggested that it may be related to differences in film preparation conditions.[28]

Similar to our previous results for PMP[6,7] and PTMSP,[8] the permeability of AF2400 is increased by FS addition. For example at $\Delta p = 3.4$ atm, methane permeability in AF2400 containing 40 wt % FS is 340% higher than that in the unfilled polymer. This result indicates that, contrary to traditional filled polymer systems where addition of nonporous fillers reduces permeability, incorporation of FS into AF2400 alters the polymer matrix to permit more rapid penetrant transport. For PMP and PTMSP this increase in penetrant flux upon FS addition was attributed to a FS-induced increase in system free volume.[6−8] On the basis of the PALS and permeation data in Figures 1 and 2, a similar effect appears to occur as FS is added to AF2400. The lack of an appreciable dependence of methane permeability on pressure exhibited in Figure 2 for both AF2400 and the nanocomposites is consistent with prior reports for this penetrant in AF2400[9] and, in general, for light gases in glassy and rubbery polymers.[11]

Previously, the enhancement in permeability induced by FS addition to PMP was shown to persist throughout a 1 month aging period in the ambient atmosphere.[7] This result suggests that FS enhanced permeability in high-free-volume polymers is relatively stable and not simply a short-lived effect. Further evidence for the stability of the FS effect is given in Table 1, which presents aging data for AF2400/FS nanocomposites. Films containing 10 and 40 wt % FS were tested after casting and then again after more than 2 years exposure to ambient conditions. For both samples, the as-cast and aged permeability coefficients are quite similar (aged values are within ±15% of as-cast values). Thus, after more than 2 years of aging, the permeability of FS-filled AF2400 was essentially unchanged and, consequently, still substantially higher than that in unfilled AF2400.

Figure 3 presents *n*-butane permeability coefficients in AF2400 and FS-filled AF2400 as a function of Δp. Similar to the methane data presented in Figure 2, the permeability of AF2400 to *n*-butane increases regularly with increasing FS content. However, unlike methane, *n*-butane permeability coefficients exhibit pressure dependence. Previously,[9,26] it was reported that AF2400 is readily plasticized by organic vapors, such as propane

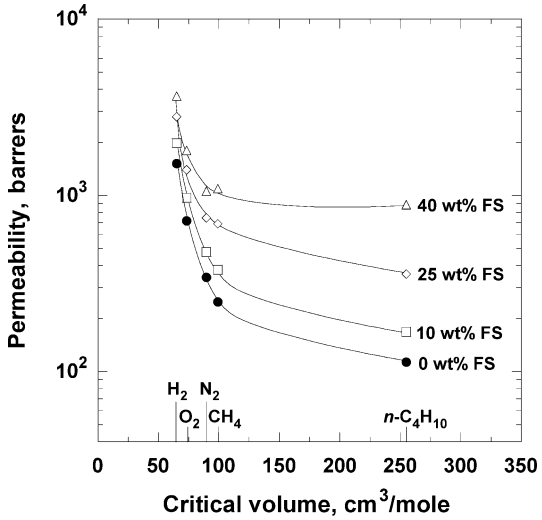

Figure 4. Permeability coefficients in AF2400 containing 0, 10, 25, and 40 wt % FS as a function of penetrant size. Data were taken at 25 °C and $\Delta p = 3.4$ atm except for *n*-butane, where Δp ranged between 0.33 and 0.44 atm (i.e., the lowest *n*-butane transmembrane pressure difference examined).

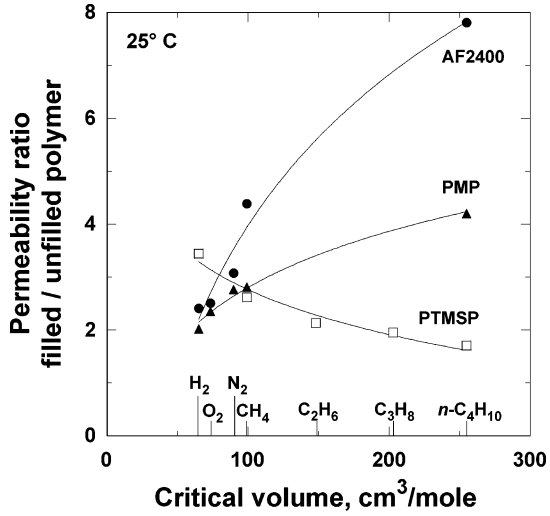

Figure 5. Permeability enhancement in AF2400, PMP, and PTMSP as a function of penetrant size. AF2400 data (●) are from pure gas measurements at 4.4 atm upstream pressure (except *n*-butane for which upstream pressure ranged from 1.3 to 1.4 atm) in AF2400 containing 40 wt % FS and pure AF2400 samples. PTMSP data (□) are taken from pure gas measurements at 4.4 atm upstream pressure (except *n*-butane for which upstream pressure = 2.1 atm) in PTMSP containing 50 wt % FS and pure PTMSP. PMP data (▲) are taken from pure gas measurements at 4.4 atm upstream pressure (except *n*-butane which is from mixed gas data at 11.2 atm upstream pressure) in PMP containing 45 wt % FS and pure PMP.

and chlorodifluoromethane. Consistent with this behavior, the permeability of AF2400 to *n*-butane measured in this work increases 3-fold over the pressure range explored. On the basis of a conventional interpretation of plasticization phenomena,[29] the insertion of relatively large *n*-butane molecules into AF2400 presumably disrupts polymer chain packing, swells the matrix (i.e., introduces additional free volume), and increases local-scale segmental dynamics, thereby increasing penetrant diffusion coefficients (which, in turn, increases permeability). As AF2400 is filled with FS, not only does *n*-butane permeability increase, but the effect of pressure on permeability changes dramatically. In contrast to AF2400, *n*-butane permeability in AF2400 containing 40 wt % FS decreases systematically with increasing Δp. This behavior is frequently observed for nonplasticizing penetrants in glassy polymers and is related to the saturation of nonequilibrium excess free volume sorption sites and resultant decrease in solubility in these polymers with increasing penetrant pressure.[29] However, it is unusual for a large, swelling-inducing penetrant like *n*-butane to exhibit such antiplasticization behavior at high penetrant activity (0.88 activity on the upstream face of the film at the highest Δp explored). Previously, in PTMSP, the amount by which *n*-butane permeability coefficients increase with increasing pressure was reduced as FS content increased.[8] Our present results for AF2400 containing FS exhibit similar, though more dramatic, behavior. This reduction in *n*-butane-induced plasticization with increasing FS content is consistent with the notion that FS addition augments the size of free volume elements in these polymers. As FS content increases, it appears to open free volume elements in AF2400 large enough to accommodate *n*-butane molecules without inducing swelling of the matrix that is typically presumed to trigger plasticization. AF2400 containing 25 wt % FS exhibits behavior intermediate between that of AF2400 and the 40 wt % FS sample, as permeability first decreases slightly and then increases with increasing transmembrane pressure difference.

Figure 4 presents pure gas permeability coefficients for a series of penetrants in AF2400 and FS-filled AF2400 as a function of molecular size, which is characterized by critical molar volume, V_C. Consistent with previous results for filled polyacetylenes, the permeability of AF2400 nanocomposites to each penetrant increases systematically with increasing FS content. For AF2400, permeability coefficients decrease regularly with increasing penetrant size, indicating that this polymer is size-selective. This permeation behavior is in contrast to that of the previously examined filled polymers (PMP and PTMSP), which are more permeable to large hydrocarbon vapors than to small permanent gases (i.e., they are vapor-selective). Thus, the creation of enhanced permeability nanocomposites via addition of FS is not limited to high-free-volume vapor-selective materials but can also be accomplished with a size-selective polymer such as AF2400. On the basis of previous results for PMP, by increasing system free volume, FS addition decreases the size-sieving capacity of this polymer, thereby enhancing vapor selectivity.[7] A similar reduction of size selectivity is observed in AF2400. For example, pure AF2400 is more permeable to smaller nitrogen than to larger, more soluble methane, while AF2400 containing 40 wt % FS is more permeable to methane than to nitrogen.

Since selectivities change upon addition of FS to AF2400, the presence of FS enhances the permeability of various penetrants to different degrees. This point is illustrated in Figure 5, where the ratio of filled to unfilled permeability coefficients in AF2400 (or permeability enhancement) is presented as a function of penetrant size. In addition to AF2400, results for PMP and PTMSP are also included. The increase in permeability due to FS addition to AF2400 becomes progressively larger as penetrant size increases. For example, hydrogen ($V_C = 65.1$ cm^3/mol) permeability is 2.4 times higher in filled AF2400 than in the unfilled polymer, but methane ($V_C = 99.2$ cm^3/mol) permeability increases 4.4 times, and the permeability of still larger *n*-butane increases nearly 8 times. This behavior is similar to that

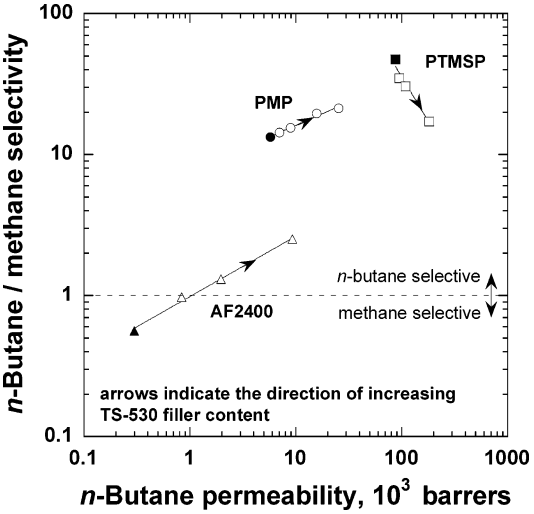

Figure 6. Mixed-gas *n*-butane/methane permselectivity vs *n*-butane permeability in AF2400 (▲), FS-filled AF2400 (Δ, 18, 30, and 40 wt %), PMP (●), FS-filled PMP (○; 15, 25, 40, and 45 wt %), PTMSP (■), and FS-filled PTMSP (□; 30, 40, and 50 wt %).

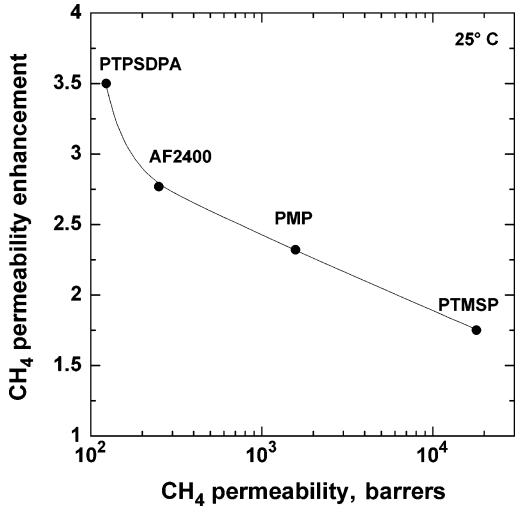

Figure 7. Methane permeability enhancement at 18 vol % TS-530 FS (i.e., ratio of filled to unfilled polymer permeability) as a function of the base polymer's unfilled methane permeability.

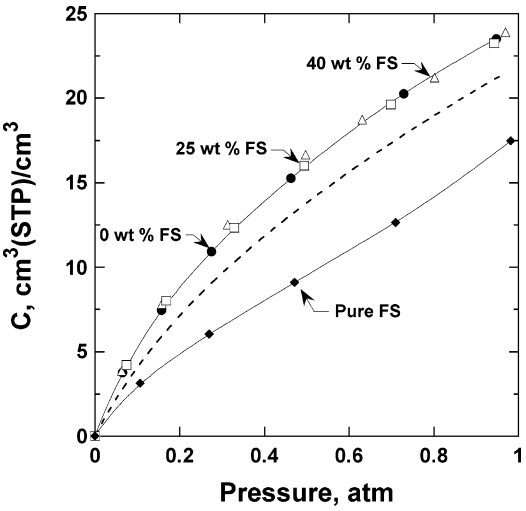

Figure 8. *n*-Butane sorption at 25 °C in AF2400 containing 0, 25, and 40 wt % FS as well as adsorption on TS-530 FS powder. The dashed line represents the predicted *n*-butane uptake by the 40 wt % FS nanocomposite based on eq 4 and the sorption capacities of pure AF2400 and TS-530 FS.

exhibited by PMP and is consistent with a reduction of diffusivity selectivity in a solution-diffusion polymer.[7] PTMSP, on the other hand, exhibits smaller permeability enhancement at larger penetrant sizes, suggesting an increased influence of free phase transport mechanisms (e.g., Knudsen diffusion).[8]

Figure 6 presents mixed-gas *n*-butane/methane selectivity as a function of mixed-gas *n*-butane permeability coefficients in AF2400 and FS-filled AF2400. Data for filled PMP and PTMSP are included in this figure for comparison. Consistent with the pure-gas data in Figure 5, both *n*-butane permeability and *n*-butane/methane selectivity increase systematically in AF2400 with increasing FS content. In fact, AF2400 exhibits a selectivity reversal; samples containing 0 and 18 wt % FS are methane selective, while those containing 30 and 40 wt % FS are *n*-butane selective. The mixed-gas behavior of filled AF2400 is similar to that of PMP and not PTMSP.[7,8] This result suggests that FS addition to AF2400 modifies polymer chain packing without creating free volume elements large enough to permit transport mechanisms that favor light gas permeation, such as Knudsen diffusion, to become important.

Previously,[6] we investigated the relative capacity of different nonporous filler particles to enhance the permeability of PMP. This analysis suggested that filler particle size might be an important parameter. Smaller primary particles were more effective at increasing permeability in PMP than larger ones. The other component in these polymer/filler systems is the polymer, and recent studies of filled polyacetylenes indicate that permeability enhancement at a given volume fraction of FS decreases as the base polymer permeability increases.[8] This result may be related to the relative free volume of the polymers being filled and their ability to accommodate FS particles within the polymer matrix. Thus, PTMSP, which possesses the largest and most numerous free volume elements among the polymers examined, accommodates FS particles with the least disruption of polymer chain packing and experiences, therefore, the smallest permeability enhancement.[8] Figure 7 demonstrates that AF2400 follows the trend exhibited by the polyacetylenes. Methane permeability enhancement at a fixed loading of FS is higher in AF2400 than it is in more permeable PMP or PTMSP but lower than the enhancement exhibited by poly(1-phenyl-2-(*p*-(triisopropylsilyl)phenyl)acetylene) [PTPSDPA], a relatively low permeability polyacetylene.

Solubility. Previously, penetrant solubility in FS-based nanocomposites of PMP and PTMSP was found to be quite similar to solubility in the filler-free polymers.[7,8] As illustrated in Figure 8, this also appears to be the case for AF2400. Within the uncertainty in the measurements, the equilibrium *n*-butane uptake in AF2400 containing 0, 25, and 40 wt % FS is equivalent. This result implies that the higher permeability of the FS-filled AF2400 samples is due to higher diffusion coefficients. *n*-Butane sorption in AF2400 and FS-filled AF2400 is higher than *n*-butane adsorption on TS-530 FS powder. However, the difference in uptake between the pure polymer and filler is much smaller for AF2400 than for the other two substituted acetylene polymers examined. For example, at 0.7 atm the amount of *n*-butane sorbed is 13, 17, 45, and 63 cm^3 (STP)/cm^3 for TS-530 FS, AF2400, PMP, and PTMSP, respectively.

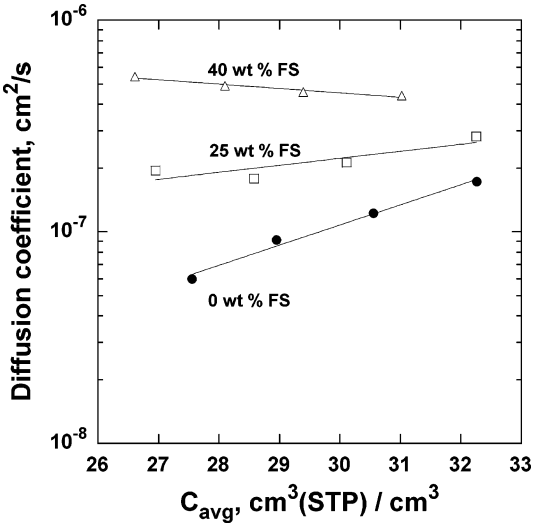

Figure 9. Concentration averaged *n*-butane diffusion coefficients in AF2400 containing 0, 25, and 40 wt % FS at 25 °C as a function of the average penetrant concentration in the film.

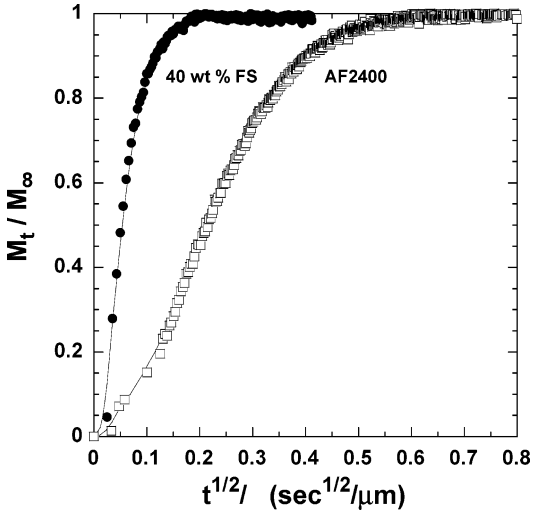

Figure 10. *n*-Butane uptake in AF2400 and AF2400 containing 40 wt % FS at 25 °C. AF2400 sample thickness = 30 μm, initial pressure = 0 Torr, final pressure = 49.5 Torr. AF2400 containing 40 wt % FS sample thickness = 40 μm, initial pressure = 0 Torr, final pressure = 48.4 Torr.

Previously, for PMP and PTMSP, sorption in the filled polymers was higher than predicted on the basis of an additive solubility model (i.e., eq 4), implying that addition of FS introduces additional accessible free volume into these systems.[7,8] The dashed line in Figure 8 represents the additive model predicted *n*-butane uptake for AF2400 containing 40 wt % FS. This predicted sorption capacity is lower than that exhibited by the 40 wt % FS nanocomposite, a result qualitatively similar to that observed in the polyacetylenes. However, as a result of the relatively small difference in *n*-butane uptake between AF2400 and TS-530 FS (as opposed to the polyacetylenes where this difference is large), the disparity in predicted (by eq 4) and measured *n*-butane sorption in AF2400 containing 40 wt % FS is close to the uncertainty in the measurements. This result simply indicates that the FS induced increase in polymer free volume is more difficult to detect via sorption measurements in AF2400 than in PMP or PTMSP.

Diffusivity. *n*-Butane equilibrium sorption and permeation data were combined to yield concentration-averaged effective diffusion coefficients, $\bar{D}$, via eq 1. Figure 9 presents these diffusion coefficients as a function of *n*-butane concentration in AF2400 containing 0, 25, and 40 wt % FS. Consistent with the permeation data and the notion that FS facilitates penetrant diffusion by opening the polymer matrix, $\bar{D}$ increases with increasing FS content in AF2400. The concentration dependence of $\bar{D}$ indicates that the degree of plasticization induced by *n*-butane decreases with increasing FS loading. In fact, while $\bar{D}$ increases with increasing *n*-butane concentration for AF2400 and AF2400 containing 25 wt % FS, it does the opposite for AF2400 containing 40 wt % FS, suggesting antiplasticization behavior in this nanocomposite. These results are consistent with FS altering AF2400 to inhibit penetrant-induced swelling, probably by augmenting the size of free volume elements relative to those in the unfilled polymer.

In addition to $\bar{D}$, which is calculated from steady-state transport data, diffusion coefficients may also be estimated from the kinetics of *n*-butane sorption. Figure 10 presents representative *n*-butane kinetic sorption fractional uptake data in AF2400 and AF2400 containing 40 wt % FS. In this figure, M_t is penetrant mass uptake at time t and M_∞ is the equilibrium mass uptake. On the basis of an inspection of Figure 10, in which *n*-butane uptake kinetics have been normalized to account for differences in film thickness, sorption equilibrium is attained much more rapidly in AF2400 containing 40 wt % FS than in AF2400. This result implies faster diffusion in the 40 wt % FS sample, and it is qualitatively consistent with the concentration averaged diffusion coefficients. For both polymer samples, the convex curvature relative to the *x*-axis at short times is a typical artifact related to a finite time being required to establish surface concentration equilibrium at the beginning of the experiment.[30] Kinetic or transient diffusion coefficients, D, may be extracted from the data in Figure 10 by application of the one-dimensional form of Fick's second law. When the mass uptake is less than 60% (i.e., $M_t/M_\infty < 0.60$) and fractional uptake is a linear function of $t^{1/2}$, D may be estimated from[31]

$$\frac{d(M_t/M_\infty)}{dt^{1/2}} = \left(\frac{16D}{l^2\pi}\right)^{1/2} \tag{7}$$

where D is, to a good approximation, an average diffusion coefficient over the concentration range corresponding to the initial and final pressures in the interval sorption experiment.[31]

Figure 11 presents *n*-butane diffusion coefficients in AF2400 and FS-filled AF2400 determined from the kinetic sorption studies. Also included in this figure are the calculated concentration-averaged diffusion coefficients ($\bar{D}$) for comparison. For each sample, kinetic diffusion coefficients (D) are measured at a lower *n*-butane concentration than $\bar{D}$ because the *n*-butane pressure (and concentration in the film) in interval sorption experiments is much lower than that in the permeation and sorption experiments used to estimate $\bar{D}$. Despite the difference in measurement and calculation technique, there is reasonable agreement between the sets of diffusion coefficients. Consistent with the FS concentration dependence of $\bar{D}$, *n*-butane kinetic diffusion coefficients increase systematically with increasing FS content. For AF2400 containing 40 wt % FS, kinetic

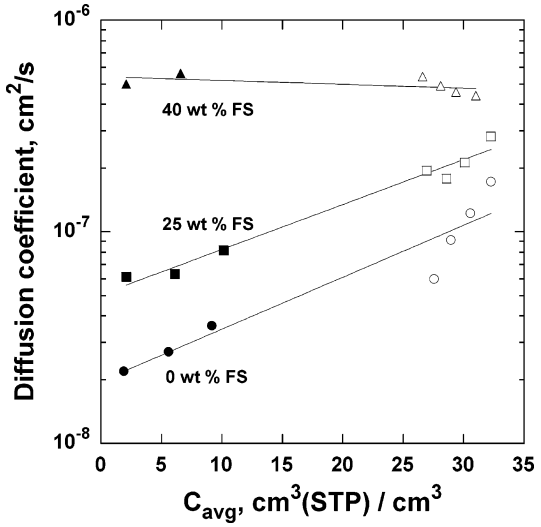

Figure 11. *n*-Butane kinetic (closed symbols) and concentration averaged (open symbols) diffusion coefficients in AF2400 containing 0, 25, and 40 wt % FS at 25 °C. The solid lines represent fits of the following model to the experimental data: $D = D_0 \exp(\beta C)$, where D_0 is an infinite dilution diffusion coefficient, β is an empirical parameter that measures the extent to which a polymer is plasticized by a penetrant, and C is the penetrant concentration in the polymer.

and concentration averaged diffusion coefficients are very similar in magnitude. This result suggests an absence of plasticization in the 40 wt % FS sample, which is consistent with *n*-butane permeation data. Additionally, the agreement between kinetic and concentration averaged diffusion coefficients is expected in nonporous films where Fick's law governs mass transport. For AF2400 and AF2400 containing 25 wt % FS, *n*-butane kinetic diffusion coefficients are significantly less than those calculated from steady-state data (i.e., $\bar{D}$). This result may reflect the fact that *n*-butane diffusion coefficients increase with increasing penetrant concentration in these two samples (recall that $\bar{D}$ is determined at a higher *n*-butane concentration than D). In fact, as demonstrated in Figure 11, a simple exponential model[32,33] for diffusion of plasticizing penetrants in glassy polymers can reasonably describe *n*-butane diffusion in AF2400 containing 0 and 25 wt % FS. The apparent plasticization of these two systems by *n*-butane is consistent with the permeation data reported earlier, while the simple relationship between D and $\bar{D}$ suggests that FS does not introduce interconnected porous pathways (i.e., defects) into the nanocomposite.

Previously, several researchers[34−36] have observed that kinetic or transient diffusion coefficients in filled polymers are greatly reduced relative to those in the unfilled polymer. Moreover, apparent diffusion coefficients in filled polymers obtained from transient measurements can be much lower than those calculated from steady-state data and are related in a complex manner.[36] These results have been attributed to immobilizing adsorption by the filler particles which increases the time required for penetrant to accumulate in the polymer system to equilibrium levels.[36] In contrast, for our AF2400/FS system, kinetic (or transient) diffusion coefficients increase with increasing filler content. In addition, steady-state diffusion coefficients can be related to transient diffusion coefficients by a simple concentration dependence model. These results are consistent with filler particles that open the polymer matrix and do not significantly immobilize *n*-butane molecules through surface adsorption or the formation of blind pores.

Conclusions

The addition of nanoscale FS particles to AF2400 has no detectable effect on the polymer's glass transition temperature, indicating that the filler has little impact on polymer chain stiffness or mobility. PALS data reveal that FS addition increases the size of free volume elements in AF2400. The enhanced free volume of filled AF2400 results in augmented penetrant permeability and diffusion coefficients, similar to behavior observed in FS-filled polyacetylenes. For the polymers examined to date, FS-induced permeability enhancement decreases with increasing base polymer permeability. The permeability of large penetrants increases more than that of small molecules in filled AF2400, consistent with a weakening of size selectivity in this polymer. As a result, AF2400 exhibits a selectivity reversal for the vapor-gas pair *n*-C_4H_{10}/CH_4, becoming *n*-butane selective above 18 wt % FS. FS addition modifies AF2400, allowing *n*-butane to be accommodated without swelling the matrix, thereby mitigating penetrant-induced plasticization, whereas unfilled AF2400 is readily plasticized by *n*-butane. Similar to previous results for PMP and PTMSP, there is no measurable effect of FS addition on penetrant solubility in AF2400. This finding implies that all of the increase in penetrant permeability in filled AF2400 is a result of increased diffusion coefficients. Kinetic diffusion coefficients from interval sorption and those calculated from equilibrium solubility and permeability data are in reasonable agreement and confirm that FS addition reduces resistance to molecular transport in AF2400.

References and Notes

(1) Paul, D. R.; Yampolskii, Y. P. *Polymeric Gas Separation Membranes*; CRC Press: Boca Raton, FL, 1994.
(2) Jia, M.; Peinemann, K. V.; Behling, R. D. *J. Membr. Sci.* **1991**, *57*, 289−296.
(3) Kulprathipanja, S.; Neuzil, R. W.; Li, N. Separation of fluids by means of mixed matrix membranes. US Patent No. 4,740,219, 1988.
(4) Mahajan, R.; Zimmerman, C. M.; Koros, W. J. In *Polymer Membranes for Gas and Vapor Separation: Chemistry and Materials Science*; Freeman, B. D., Pinnau, I., Eds.; American Chemical Society: Washington, DC, 1999; pp 277−286.
(5) Pinnau, I.; He, Z. Filled Superglassy Membrane. U.S. Patent No. 6,316,684, 2001.
(6) Merkel, T. C.; Freeman, B. D.; Spontak, R. J.; He, Z.; Pinnau, I.; Meakin, P.; Hill, A. J. *Science* **2002**, *296*, 519−522.
(7) Merkel, T. C.; Freeman, B. D.; He, Z.; Pinnau, I.; Meakin, P.; Hill, A. J. *Chem. Mater.* **2003**, *15*, 109−123.
(8) Merkel, T. C.; Freeman, B. D.; He, Z.; Pinnau, I.; Meakin, P.; Hill, A. J. *Macromolecules* **2003**, *36*, 6844−6855.
(9) Merkel, T. C.; Bondar, V. I.; Nagai, K.; Freeman, B. D.; Yampolskii, Y. *Macromolecules* **1999**, *32*, 8427−8440.
(10) Koros, W. J.; Fleming, G. K.; Jordan, S. M.; Kim, T. H.; Hoehn, H. H. *Prog. Polym. Sci.* **1988**, *13*, 339−401.
(11) Ghosal, K.; Freeman, B. D. *Polym. Adv. Technol.* **1994**, *5*, 673−697.
(12) Barrer, R. M. In *Diffusion in Polymers*; Crank, J., Park, G. S., Eds.; Academic Press: London, 1968; pp 165−217.
(13) van Amerongen, G. J. *Rubber Chem. Technol.* **1964**, *37*, 1065−1152.
(14) Barrer, R. M.; Barrie, J. A.; Raman, N. K. *Polymer* **1962**, *3*, 605−614.
(15) CAB-O-SIL TS-530 Treated Fumed Silica: Technical Data, Cabot Corp., 1991.
(16) Stern, S. A.; Gareis, P. J.; Sinclair, T. F.; Mohr, P. H. *J. Appl. Polym. Sci.* **1963**, *7*, 2035−2051.
(17) Resnick, P. R.; Buck, W. H. Teflon AF Amorphous Fluoropolymers. In *Modern Fluoropolymers: High Performance*

Polymers for Diverse Applications; Scheirs, J., Ed.; John Wiley & Sons: New York, 1997; pp 397−419.
(18) Tong, S. N.; Chen, M. L.; Wu, P. In *Analysis of Transition Temperatures in Polymer-Filler Systems*; Mitchel, J., Ed.; Oxford University Press: New York, 1992; Vol. 2, pp 329−345.
(19) Iisaka, K.; Shibayama, K. *J. Appl. Polym. Sci.* **1978**, *22*, 3135−3143.
(20) Yim, A.; Chahal, R. S.; Pierre, L. E. S. *J. Colloid Interface Sci.* **1973**, *43*, 583−590.
(21) Hergeth, W. D.; Steinau, U. J.; Bittrich, H. J.; Simon, G.; Schmutzler, K. *Polymer* **1989**, *30*, 254−258.
(22) Lipatov, Y. S.; Fabulyak, F. G. *J. Appl. Polym. Sci.* **1972**, *16* (8), 2131−2139.
(23) Yampol'skii, Y. P.; Shantorovich, V. P.; Chernyakovskii, F. P.; Kornilov, A. I.; Plate, N. A. *J. Appl. Polym. Sci.* **1993**, *47*, 85−92.
(24) Consolati, G.; Genco, I.; Pegoraro, M.; Zanderighi, L. *J. Polym. Sci., Polym. Phys. Ed.* **1996**, *34*, 357−367.
(25) Nemser, S. M.; Roman, I. A. Perfluorodioxole Membranes. U.S. Patent No. Patent 5,051,114, 1991.
(26) Pinnau, I.; Toy, L. G. *J. Membr. Sci.* **1996**, *109*, 125−133.
(27) Pauly, S. In *Polymer Handbook*, 3rd ed.; Brandrup, J., Immergut, E. H., Eds.; John Wiley & Sons: New York, 1989.
(28) Alentiev, A. Y.; Yampolskii, Y. P.; Shantarovich, V. P.; Nemser, S. M.; Plate, N. A. *J. Membr. Sci.* **1997**, *126*, 123−132.
(29) Koros, W. J.; Hellums, M. W. In *Encyclopedia of Polymer Science and Technology*; Kroschwitz, J. I., Ed.; 1990; p 724−802.
(30) Morisato, A.; Miranda, N. R.; Freeman, B. D.; Hopfenberg, H. B.; Costa, G.; Grosso, A.; Russo, S. *J. Appl. Polym. Sci.* **1993**, *49*, 2065−2074.
(31) Crank, J. *The Mathematics of Diffusion*, 2nd ed.; Clarendon Press: Oxford, 1975.
(32) Stern, S. A.; Saxena, V. *J. Membr. Sci.* **1980**, *7*, 47−59.
(33) Zhou, S.; Stern, S. A. *J. Membr. Sci.* **1989**, *27*, 205−222.
(34) Higuchi, W. I.; Higuchi, T. *J. Am. Pharm. Assoc.: Sci. Ed.* **1960**, *49*, 598−606.
(35) Most, C. F. *J. Appl. Polym. Sci.* **1970**, *14*, 1019−1024.
(36) Paul, D. R.; Kemp, D. R. *J. Polym. Sci., Polym. Symp.* **1973**, *41*, 79−93.

MA034975Q